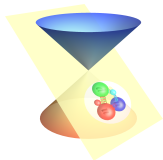


Hamiltonian Approach to Quantum Field Theories on the Light Front

Yang Li

Department of Physics and Astronomy,
Iowa State University, Ames, IA, U.S.




Working Month 2016



Beijing, Hefei, Nanjing, Shanghai, June 1–25, 2016



Résumé: Yang Li (李 阳)

Birth: September, 1987, Hebei

Contact:  leeyoung@iastate.edu, leeyoung1987@gmail.com

   @AichiLee

Education:

- B.S. in Physics, 2010, **University of Science and Technology of China**, Hefei, China
 - GPA: 3.80/4.3 (Theoretical Physics)
 - Research Areas: Quantum Measurement, Computational Physics
- Ph.D. in Nuclear Physics, 2015, **Iowa State University**, Ames, IA, U.S.
 - Dissertation: *Ab initio* approach to quantum field theories on the light front
 - Ph.D. Advisors: James P. Vary, Kirill Tuchin (co-major professor)
 - Research Areas: Non-Perturbative QCD, Hadronic Physics



Experience:

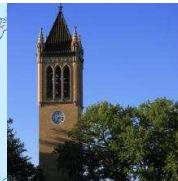
- 2016 –, **Postdoctoral Research Associate**
 - Iowa State University, Ames, IA, U.S.

Teaching:

- 2010 – 2012, 2016: **Teaching Assistant**



Nuclear Theory Group at Iowa State



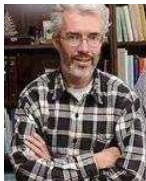
Faculty:



James P. Vary



Kirill Tuchin



Pieter Maris



Jian-wei Qiu (Emeritus)



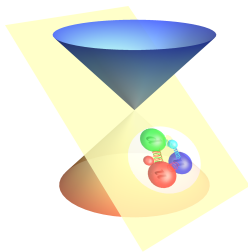
Outline

- Light-front Hamiltonian formalism
- Basis light-front quantization
- Non-perturbative renormalization
- Summary and outlooks



Part I:

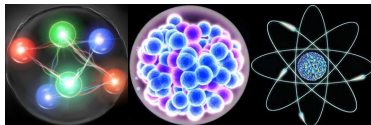
Introduction to Light-Front QCD



Introduction



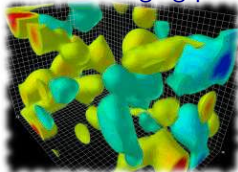
QFT
⇒



Solving QCD in the non-perturbative regime from first principles is one of the central tasks in nuclear physics

- ▶ quantum chromodynamics is the underlying theory of strong interaction
- ▶ features: asymptotic freedom, confinement, chiral symmetry breaking
- ▶ mass spectroscopy and structures of hadrons, deriving realistic nuclear forces, useful tool for Standard Model and beyond, ...

Ab initio calculation of quantum field theory (QFT) remains one of the most challenging problems in theoretical and computational physics.



Yang Li, Iowa State U, June 3, 2016



6/1



Working Month 2016, Beijing, China



Non-Perturbative Approaches

Lagrangian formalism

Euclidean space

correlators: $\langle \mathcal{O}(x_1, \dots, x_n) \rangle$

$$\langle \mathcal{O} \rangle = \int \mathcal{D}_\psi \mathcal{O} \exp \left(- S_E[\psi] \right)$$

—

Lattice QCD, DS/BSE

advantages: covariant,
tamed gauge symmetry

Hamiltonian formalism

Minkowski space

wavefunctions: $|\psi_h\rangle$

$$H|\psi_h\rangle = E_h|\psi_h\rangle$$

$$i \frac{\partial}{\partial t} |\psi_h(t)\rangle = H|\psi_h(t)\rangle$$

DLCQ, BLFQ, Transverse Lattice

advantages: Lorentzian (DIS),
access to distributions, real-time

The Hamiltonian and Lagrangian approaches are complementary to each other.

“Quantum field theory is the way it is because it is the only way to reconcile the principles of quantum mechanics with those of special relativity.”

— S. Weinberg, *The Quantum Theory of Fields*



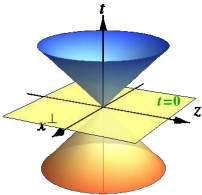
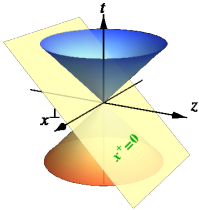
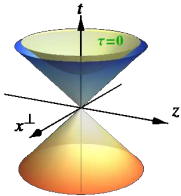
Dirac's Forms of Relativistic Dynamics

[Dirac, Rev.Mod.Phys. '49]

Due to relativity, we have the liberty to choose the direction of the dynamical evolution.

Dirac's front form gives maximal number of kinematical operators (7/10).

$$P^\pm \triangleq P^0 \pm P^3, \vec{P}^\perp \triangleq (P^1, P^2), x^\pm \triangleq x^0 \pm x^3, \vec{x}^\perp \triangleq (x^1, x^2), E^i = M^{+i}, E^+ = M^{+-}, F^i = M^{-i}, K^i = M^{0i}, J^i = \frac{1}{2}\epsilon^{ijk} M^{jk}.$$

	<u>instant form</u>	<u>front form</u>	<u>point form</u>
time variable	$t = x^0$	$x^+ \triangleq x^0 + x^3$	$\tau \triangleq \sqrt{t^2 - \vec{x}^2 - a^2}$
quantization surface			
Hamiltonian	$H = P^0$	$P^- \triangleq P^0 - P^3$	P^μ
kinematical	\vec{P}, \vec{J}	$\vec{P}^\perp, P^+, \vec{E}^\perp, E^+, J_z$	\vec{J}, \vec{K}
dynamical	\vec{K}, P^0	\vec{F}^\perp, P^-	\vec{P}, P^0
dispersion relation	$p^0 = \sqrt{\vec{p}^2 + m^2}$	$p^- = (\vec{p}_\perp^2 + m^2)/p^+$	$p^\mu = mv^\mu \ (v^2 = 1)$



Light-Front Dynamics

[Reviews: e.g. Burkardt '96, Carbonell '98, Brodsky '98]

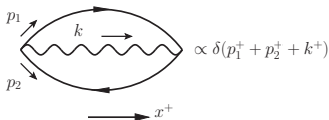
Light-front quantization defines a system on the light front $t + z/c = 0$.

- ▶ light-front energy: p^- , momenta: (p^+, p^1, p^2) , where $p^\mp = p^0 \mp p^3$
- ▶ dispersion relation (cf. non-relativistic dispersion relation)

$$p^\mu p_\mu = m^2 \Rightarrow \begin{cases} p^0 = \sqrt{\vec{p}^2 + m^2}, & \text{equal-time} \\ p^- = (\vec{p}_\perp^2 + m^2)/p^+, & \text{light-front} \end{cases}$$

- ▶ spectral condition: $p^+ \geq 0, p^- \geq 0$

[Leutwyler '78]

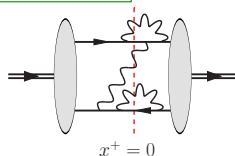


Implication:

light-front vacuum is simple!!

Dynamical evolution in x^+ direction ($x^+ = x^0 + x^3$):

$$i \frac{\partial}{\partial x^+} |\psi(x^+)\rangle = \frac{1}{2} \hat{P}^- |\psi(x^+)\rangle.$$



Hadron spectroscopy and light-front wavefunctions:

$$(P^+ \hat{P}^- - \vec{P}_\perp^2) |\psi_h\rangle = M_h^2 |\psi_h\rangle.$$



Fock Space Representation

LFD is particularly suitable for Fock space expansion:

- ▶ intuitive picture;
- ▶ vacuum pair production/annihilation is suppressed;
- ▶ all three boost transformations are kinematical;

$$|\psi_h(P, j, \lambda)\rangle = \sum_{n=1}^{\infty} \int dD_n \psi_{h/n}(\{\vec{k}_{i\perp}, x_i, \lambda_i\}_n) |\{p_i, \lambda_i\}_n\rangle$$

The Fock sector projections $\psi_{h/n}(\{\vec{k}_{i\perp}, x_i, \lambda_i\}_n) = \langle \{p_i, \lambda_i\}_n | \psi_h \rangle$ are called the *light-front wavefunctions (LFWFs)*.

In Fock space, QFT becomes a many-body problem.

By working with $H_{\text{LC}} \equiv P_\mu P^\mu = P^+ \hat{P}^- - \vec{P}_\perp^2$ we only need to deal with the relative degrees of freedom.

LFWFs describes the intrinsic structure of hadrons.

[Brodsky '98]

Thanks to the kinematical nature of LFD, the LFWFs are **frame-independent** (**boost invariant**) and only depend on the intrinsic (boost-invariant) momenta.

$$x_i \equiv p_i^+ / P^+, \quad \vec{k}_{i\perp} \equiv \vec{p}_{i\perp} - x_i \vec{P}_\perp \implies \sum_i x_i = 1, \quad \sum_i \vec{k}_{i\perp} = 0.$$

“Hadron Physics without LFWFs is like Biology without DNA!”

— Stanley J. Brodsky



Light-Front Wavefunctions

LFWFs provides intrinsic information of the structure of hadrons:

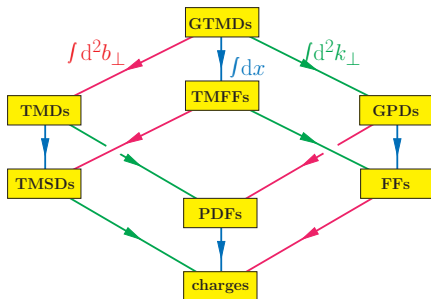
- ▶ Structure functions are the square of LFWFs
- ▶ Form factors (e.m., gravitational ...) are the overlap of LFWFs

$$A(q^2) = \sum_n \int dD_n \sum_{f=1}^n x_f \psi_n^* (\{\vec{k}'_{i\perp}, x_i, \lambda_i\}_f) \psi_n (\{\vec{k}_{i\perp}, x_i, \lambda_i\}_f)$$

$$\vec{k}'_{i\perp} = \begin{cases} \vec{k}_{i\perp} + (1 - x_i) \vec{q}_{\perp}, & \text{for struck partons} \\ \vec{k}_{i\perp} - x_i \vec{q}_{\perp}, & \text{for spectators.} \end{cases}$$

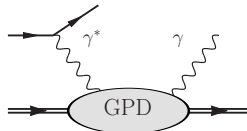
- ▶ Distributions (hadron tomography)

[Ji '97&'98]



$$\vec{k}_{\perp} \leftrightarrow \vec{r}_{\perp}, \vec{\Delta}_{\perp} \leftrightarrow \vec{b}_{\perp}$$

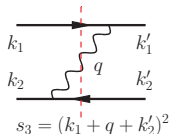
[Lorce & Pasquini '11]



- ▶ LFWFs are indispensable for exclusive processes in DIS

Hamiltonian perturbation theory: x^+ -ordered diagrams

- ▶ all particles are on their mass-shells $p_i^2 = m_i^2$;
- ▶ longitudinal and transverse momenta are conserved at each vertex;
 $\delta(\sum_i p_i^+ - P^+) \Leftrightarrow \delta(\sum_i -1)$; $\delta^2(\sum_i \vec{p}_{i\perp} - \vec{P}_\perp) \Leftrightarrow \delta^2(\sum_i \vec{k}_{i\perp})$
- ▶ the light-front energy is *not conserved* ("off the energy shell");
- ▶ energy denominator for intermediate states;



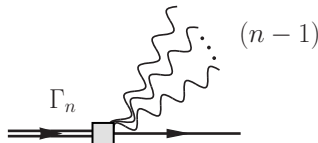
$$\frac{1}{s_n - M^2}, \quad s_n \equiv (k_1 + \dots + k_n)^2 = \sum_{a=1}^n \frac{\vec{k}_{a\perp}^2 + m_a^2}{x_a},$$

M is the mass eigenvalue

Extended to non-perturbative regime by introducing vertex functions Γ_n

$$\Gamma_n = (s_n - M^2)\psi_n.$$

Γ_n are also boost invariants.



Example:

Diagrammatic equations illustrating the renormalization of a fermion propagator:

$$\begin{aligned}
 & \text{Bare propagator } \Gamma_1 = \text{Self-energy } \delta m^2 + \text{One-loop self-energy } g_B \\
 & \text{One-loop self-energy } \Gamma_2 = \text{One-loop counterterm } g_B + \text{Two-loop self-energy } \delta m^2 \\
 & \text{Two-loop self-energy } \Gamma_3 = \text{Two-loop counterterm } g_B + \text{Three-loop self-energy } g_B \\
 & \text{Three-loop self-energy } \Gamma_4 = \text{Three-loop counterterm } g_B + (a \leftrightarrow b) + (a \leftrightarrow c)
 \end{aligned}$$



Light-Front QCD within Light-Cone Gauge ($A^+ = 0$)

$$\mathcal{L}_{\text{YM}} = -\frac{1}{4}F_{\mu\nu c}F^{\mu\nu c} + \bar{\psi}(i\not{D} - m)\psi$$

\Downarrow

light-front quantization in light-cone gauge

[Dirac '56, Brodsky '98]

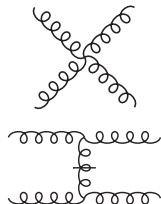
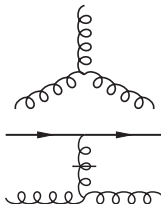
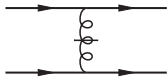
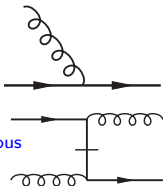
\Downarrow

$$P_{\text{LFQCD}}^- = \frac{1}{2} \int d^3x \left[\underbrace{\bar{\psi} \gamma^+ \frac{(i\partial^\perp)^2 + m^2}{i\partial^+} \psi + A_a^i (i\partial^\perp)^2 A_a^i}_{\text{kinetic energy}} \right] + P_{\text{int}}^-.$$

interaction vertices: P_{int}^-

dynamical

instantaneous



QED & QCD vertices

QCD vertices

Renormalization

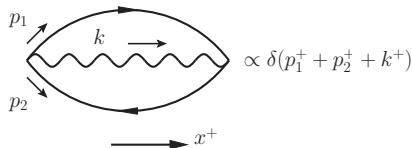
- QFT is defined with bare parameters (equivalently, counterterms). Renormalization relates these bare parameters to “physical” quantities. The bare parameters may contain divergences which is allowed as they are not physical observables.
- Renormalization depends on the regularization scheme. Infinities may arise and the theory has to be regularized first.
- After renormalization, the theory should be free of divergences in *all sectors* (e.g. bound states) even in the non-perturbative regime. Ensuring exactly cancellation of divergences (within the numerical precision) in the non-perturbative regime is often a challenge as finding the solutions often relies on numerical procedures.
- **Mass renormalization:** imposing the physical mass $M \rightarrow m_{\text{ph}}$
- **Coupling constant renormalization:** imposing the physical coupling on the vertex $\Gamma_2(\vec{k}_\perp^*, x^*) = g_{\text{ph}} \sqrt{Z}$ at some chosen kinematic point (\vec{k}^*, x^*) or s^* .
- **Wavefunction renormalization:** simply the normalization of the LFWFs! $\sum_n \int dD_n |\psi_n|^2 = 1$



Advantages of Light-Front Dynamics

[Bakker '13]

- ☺ Non-perturbative based on first principles in Minkowski space;
It provides access to real-time information of the quantum system.
- ☺ Light-front boost transformations are kinematical;
In particular, LFWFs are boost invariant, i.e., frame independent.
light-front wavefunction \neq equal-time wavefunction in rest frame [see e.g. Järvinen '05]
- ☺ LFWFs provide *intrinsic information* of the structure of the system;
 - ☺ structure functions are the square of LFWFs [Lepage '80]
 - ☺ form factors are the overlap of LFWFs
- ☺ Light-front vacuum is simple;



- ☺ Light-front kinetic energy resembles the non-relativistic one;
IF: $M^2 = \left(\sum_i \sqrt{\vec{p}_i^2 + m_i^2} \right)^2 - \vec{P}^2$; FF: $M^2 = \sum_i \frac{\vec{p}_{i\perp}^2 + m_i^2}{x_i} - \vec{P}_\perp^2$.
- ☺ Light-front dynamics is directly related to the infinite momentum frame in deep inelastic scattering.



Challenges in Light-Front Dynamics

☹ Transverse rotations are dynamical;

[see, e.g., Carbonell '98]

$$P^2|\psi_h(p, s, \lambda)\rangle = M_h^2|\psi_h(p, s, \lambda)\rangle,$$
$$\vec{S}^2|\psi_h(p, s, \lambda)\rangle = s(s+1)|\psi_h(p, s, \lambda)\rangle$$

spin operator: $\vec{S}^2 = -W^2/P^2$, $W^\mu = -\frac{1}{2}\varepsilon^{\mu\nu\rho\sigma}M_{\nu\rho}P_\sigma$.

☹ Fock sectors are not gauge invariants;

☹ Zero-mode issue: $p_i^+ = 0$;

LFQCD often offers a drastically different physical picture from Lagrangian formalism.

[e.g. Brodsky '10]

“Light-front QCD is not for the faint of heart, but for a few good candidates it is a chance to be a leader in a much smaller community of researchers than one faces in the major areas of high-energy physics, with, I believe, unusual promise for interesting and unexpected results.” — Kenneth G. Wilson, *The Origins of Lattice Gauge Theory*, 2005



Some Perspectives on Non-Perturbative LQCD

LF Tamm-Dancoff coupled integral equations

[Perry '90]

- ▶ systematic Fock sector truncation with sector dependent renormalization schemes. [see, e.g., YL et al. Phys.Lett.B '15]
- ▶ wave-equation/few-body approach [Hiller, Karmanov, Chabysheva, Li]

Direct diagonalization: large sparse matrix eigenvalue problem

- ▶ many-body approach: DLCQ, BLFQ, ... [e.g., Pauli '89, Vary '10]
- ▶ in parallel with *ab initio* nuclear structure calculations [Barrett '13]
configuration interaction, Green function Monte-Carlo, coupled cluster ...
- ▶ need effective eigensolvers suitable for HPC [work in progress!]

Collective modes

[e.g., Vary '05, Misra '00, More '12, Chabysheva '12]

- ▶ coherent basis, LF coupled cluster, ...

Transverse lattice

[Burkardt, Dalley, Van de Sande, Chakrabarti]

Effective operator

[Wilson, Głazek, Perry]

- ▶ Bloch method [Wilson '76]
- ▶ flow equation/similarity renormalization group (SRG) [Głazek '94]

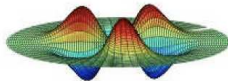
Holographic light-front QCD

[Brodsky '06]



Part II:

Basis Light-Front Quantization



Hamiltonian light-front field theory in a basis function approach

J. P. Vary,¹ H. Honkanen,¹ Jun Li,¹ P. Maris,¹ S. J. Brodsky,² A. Harindranath,³ G. F. de Teramond,⁴ P. Sternberg,^{5,*}
E. G. Ng,⁵ and C. Yang⁵

Discretized Light Cone Quantization

Pauli & Brodsky c1985

**Basis Light Front Quantization***

$$\phi(\vec{x}) = \sum_{\alpha} [f_{\alpha}(\vec{x}) a_{\alpha}^{+} + f_{\alpha}^{*}(\vec{x}) a_{\alpha}]$$

where $\{a_{\alpha}\}$ satisfy usual (anti-) commutation rules.

Furthermore, $f_{\alpha}(\vec{x})$ are arbitrary except for conditions:

Orthonormal: $\int f_{\alpha}(\vec{x}) f_{\alpha'}^{*}(\vec{x}) d^3x = \delta_{\alpha\alpha'}$

Complete: $\sum_{\alpha} f_{\alpha}(\vec{x}) f_{\alpha}^{*}(\vec{x}') = \delta^3(\vec{x} - \vec{x}')$

=> Wide range of choices for $f_{\alpha}(\vec{x})$ and our initial choice is

$$f_{\alpha}(\vec{x}) = N e^{ik^{+}x^{-}} \Psi_{n,m}(\rho, \varphi) = N e^{ik^{+}x^{-}} f_{n,m}(\rho) \chi_m(\varphi)$$



Steps to implement Basis Light-Front Quantization

- ▶ Enumerate Fock space basis subject to symmetry constraints and regularizations; (keep the bookkeeping under control: cf. No-Core Shell Model)
- ▶ Evaluate the LC Hamiltonian operator H_{LC} in that basis;
- ▶ Diagonalization (Lanczos, QR, ...);
- ▶ Evaluate observables using LFWFs;
- ▶ Repeat previous steps for new regulators, and extrapolate to continuum limit.

Above achieved for QED test cases — electron in a trap

H. Honkanen, P. Maris, J.P. Vary, S.J. Brodsky, Phys. Rev. Lett. 106, 061603 (2011)

Improvements for QED test cases: trap independence, renormalization, ...

X. Zhao, H. Honkanen, P. Maris, J.P. Vary, S.J. Brodsky, Phys. Lett. B 737, 65 (2014)

Positronium at strong coupling in harmonic oscillator basis: (first bound-state application)

P. Wiecki, YL, X. Zhao, P. Maris, J.P. Vary, Phys. Rev. D 91, 105009 (2015)

Heavy Quarkonium in a Holographic basis:

YL, P. Maris, X. Zhao, J.P. Vary, Phys. Lett. B 758, 118 (2016)



Symmetries and Constraints

Symmetries & Constraints

$$\sum_i b_i = B$$

$$\sum_i e_i = Q$$

$$\sum_i (m_i + s_i) = J_z$$

$$\sum_i k_i = K$$

$$\sum_i [2n_i + |m_i| + 1] \leq N_{\max}$$

Global Color Singlets (QCD)

Light Front Gauge

Optional - Fock space cutoffs

$$H \rightarrow H + \lambda H_{CM}$$

All $J \geq J_z$ states obtained
in a single calculation

Finite basis regulators

Thanks to the kinematical nature of
light-front boost transformation and
consistent choice of basis and
truncation.



- ▶ BLFQ adopts basis function expansion and basis regularization.
Optimal basis is the key to numerical efficiency. The basis functions can be chosen to approximate the solution (e.g. AdS/QCD basis).
- ▶ BLFQ exploits the kinematic symmetries of the Hamiltonian.
especially: preserves J_z while allows separation of center of mass motion
- ▶ BLFQ is designed as a many-body method in parallel with the configuration interaction (CI) method in strong coupling non-relativistic many-body problems.
We can learn from non-relativistic many-body problems.
- ▶ BLFQ yields large sparse matrix eigenvalue problems, which need to be solved with modern high performance computing (HPC).
- ▶ Time-dependent Basis Light-Front Quantization (tBLFQ). [Zhao '13]

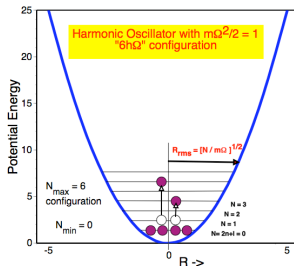
Key insight: nonrelativistic and light-front Hamiltonian problems have much in common. We need effective eigensolvers suitable for modern HPC, similar to e.g., many-fermion dynamics (MFDn) in No-Core Shell Model (NCSM).



What motivates this BLFQ approach?

- Exact treatment of all symmetries (dynamical & kinematical)
- Success in ab-initio nuclear many-body theory (equal time, non-relativistic)
- High precision results from No-Core Full Configuration (NCFC) approach
- Advances in solving sparse matrix problems on parallel computers
- Growth in the size/capacity of parallel computers

Parameters of
the HO basis space



Electron

[Honkanen '10, Zhao '14, cf. Hiller and Brodsky '98]

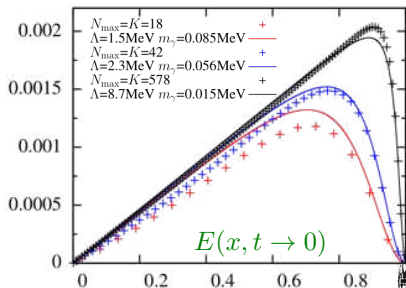
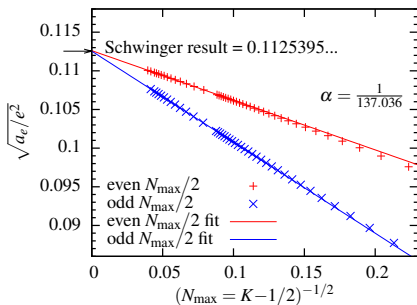
Physical electron is obtained from diagonalizing the (regularized & truncated) QED Hamiltonian in the single-electron sector.

$$|e_{\text{ph}}\rangle = |e\rangle + |e\gamma\rangle + |e\gamma\gamma\rangle + |ee\bar{e}\rangle + |ee\bar{e}\gamma\rangle \dots$$

Truncation up to $e\gamma$ is equivalent to 1-loop QED correction. Note that BLFQ provides the electron wavefunction.

Electron AMM (a_e) — a benchmark calculation for QFT:

$$\frac{q_1 - iq_2}{2m_e} F_2(q^2) = \langle e_{\text{ph}}(p+q), \uparrow | J^+(0) | e_{\text{ph}}(p), \downarrow \rangle, \quad (a_e = F_2(0))$$



Largest calculation with basis dimension > 28 billion

Positronium

[Wiecki, YL, Zhao, Maris, Vary PRD 91, 105009 (2015)]

- Positronium is a gold-plated bound-state system in QFT.
- Positronia are obtained from diagonalizing the (regularized & truncated) QED Hamiltonian in the $e\bar{e}$ sector.

$$|Ps\rangle = |e\bar{e}\rangle + |e\bar{e}\gamma\rangle + |\gamma\rangle + |e\bar{e}\gamma\gamma\rangle + |e\bar{e}e\bar{e}\rangle + |e\bar{e}e\bar{e}\gamma\rangle \dots$$

- one-photon exchange: neglecting the annihilation vertex
 - use an artificially large coupling $\alpha = 0.3$
- Effective Hamiltonian approach is employed where H_{eff} is obtained from Bloch method with perturbative expansion.

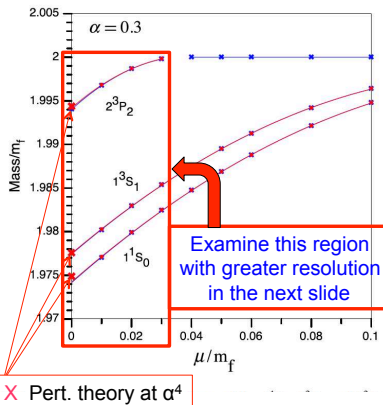
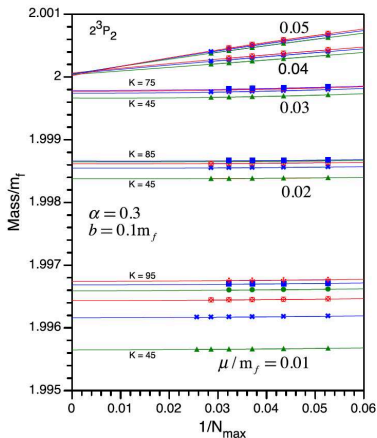
[Krautgartner '93, Trittman '97, Lamm '14, Wiecki '15]

$$H_{\text{eff}} = \text{[diagram 1]} + \text{[diagram 2]} + \text{[diagram 3]}$$

- The theory is solved in the single-particle 2D HO + 1D DLCQ basis to demonstrate the scalability (esp. separation of c.m. motion).
- Extensive extrapolation is employed to reach the continuum limit.



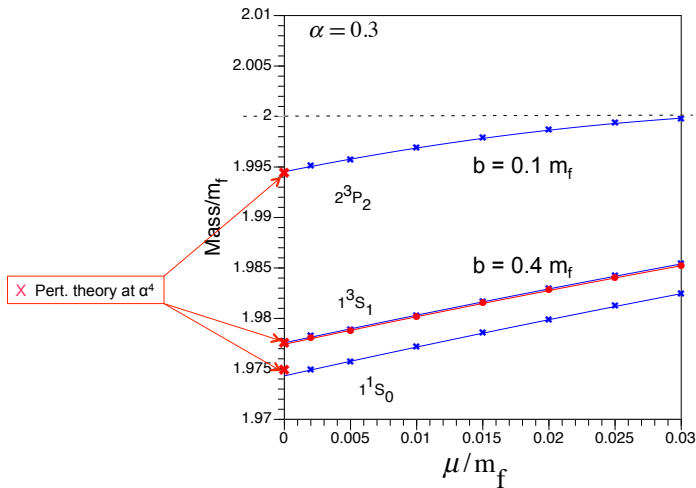
Positronium in QED at Strong Coupling Covariant Basis Light-Front Quantization (BLFQ)



P. Wiecki, Y. Li, X. Zhao, P. Maris and J.P. Vary, Phys. Rev. D **91**, 105009 (2015)



Positronium in QED at Strong Coupling Covariant Basis Light-Front Quantization (BLFQ)



P. Wiecki, Y. Li, X. Zhao, P. Maris and J.P. Vary, Phys. Rev. D **91**, 105009 (2015); & to be published



Generalized parton distributions (GPDs)

[Ji '97 & '98]

$$H(x, \zeta, t) = \frac{1}{2} \int \frac{dz^-}{2\pi} e^{ixP^+z^-} \langle P' | \bar{\psi}(-\frac{1}{2}z) \gamma^+ \psi(+\frac{1}{2}z) | P \rangle \Big|_{z^+ = z^\perp = 0}$$

$$q = P' - P, \zeta = q^+/P^+, t = q^2.$$

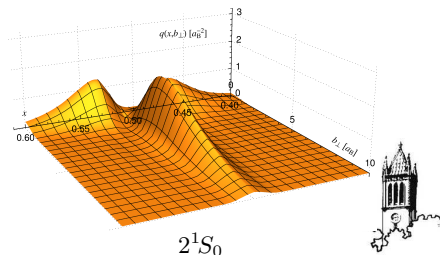
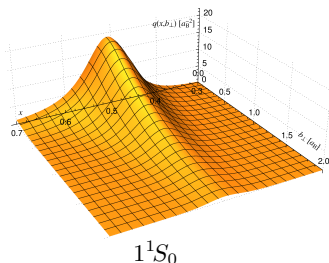
Impact parameter dependent GPDs:

[Burkardt '01]

$$q(x, \vec{b}_\perp) = \int \frac{d^2\Delta_\perp}{(2\pi)^2} e^{i\vec{\Delta}_\perp \cdot \vec{b}_\perp} H(x, \zeta = 0, t = -\Delta_\perp^2).$$

- ▶ partonic interpretation: $\int d^2b_\perp \int_0^1 dx |q(x, \vec{b}_\perp)|^2 = 1.$
- ▶ Light-front wavefunction representation

[Brodsky '01, Diehl '03]



Heavy Quarkonium

First application of BLFQ to QCD bound-state problems



Ideal laboratory to study the interplay between perturbative and non-perturbative QCD.

[Brambilla '11]

- ▶ extensive experimental measurements: BaBar, Belle, CLEO, LHC ...
- ▶ many mysteries: XYZ, quark-gluon hybrids, ...
- ▶ important for: hadron reactions, SM parameters, ...

Physical picture:

[e.g., Eichten '75, Godfrey '83]

- ▶ non-relativistic potential model: confinement plus Coulomb;
- ▶ relativity necessary for getting the hyperfine structure;

Theoretical approaches:

[Brambilla '14]

Lattice QCD, Effective Field Theory, Dyson-Schwinger/Bethe-Salpeter Equation, Constituent Quark Model, ...



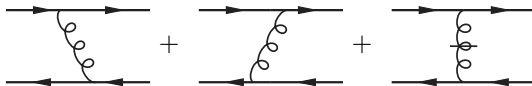
Effective Hamiltonian I

[YL et al., Phys.Lett.B 758, 118 (2016)]

Effective one-gluon exchange from the Bloch method:

[Wilson '74]

$$|\psi_{h/q\bar{q}}\rangle = |q\bar{q}\rangle + |q\bar{q}g\rangle + |q\bar{q}gg\rangle + |q\bar{q}q\bar{q}\rangle + |q\bar{q}q\bar{q}g\rangle + \dots$$



$$H_{\text{eff}} = \mathcal{P}H_0\mathcal{P} + \mathcal{P}H\mathcal{Q} \frac{1}{\frac{1}{2}(\epsilon_i + \epsilon_f) - \mathcal{Q}H_0\mathcal{Q}} \mathcal{Q}H\mathcal{P}$$

Bloch Hamiltonian is based on weak coupling expansion, which is only justified at short-distance.

For long-distance physics, we adopt a confining potential inspired by light-front holographic QCD

[Brodsky '06]

$$V(\zeta_{\perp}) = \kappa^4 \zeta_{\perp}^2 + \text{const.} \quad (\zeta_{\perp} = \sqrt{x(1-x)}r_{\perp})$$

- ▶ AdS/QCD: first approximation to QCD inspired by AdS/CFT
- ▶ soft-wall AdS/QCD produces Regge trajectory
- ▶ LF holography relates AdS/QCD to LF Schrödinger equation
- ▶ successful applications: spectrum, form factors, β -function, ...

[Karch '06]



Effective Hamiltonian II

[YL et al., Phys.Lett.B **758**, 118 (2016)]

Quark masses and longitudinal dynamics:

- ▶ Soft-wall confinement is purely transverse and were derived for massless quarks

- ▶ Invariant mass *ansatz*: $\frac{\vec{k}_\perp^2}{x(1-x)} \rightarrow \frac{\vec{k}_\perp^2 + m_q^2}{x} + \frac{\vec{k}_\perp^2 + m_{\bar{q}}^2}{1-x}$ [Brodsky '08]

We proposed a longitudinal confinement:

- ▶ It generates distribution amplitudes that match pQCD asymptotics:

$$\chi_\ell(x) \sim x^\alpha (1-x)^\beta P_\ell^{(\alpha,\beta)}(2x-1), \quad P_\ell^{(a,b)} \text{ Jacobi polynomial}$$

- ▶ In massless limit, it restores the soft-wall model
- ▶ In nonrelativistic limit, it sits on equal footing with the transverse confinement

transverse & longitudinal confinements form a 3D HO potential

- ▶ No extra free parameters

$$H_{\text{eff}} = \underbrace{\frac{\vec{k}_\perp^2 + m_q^2}{x} + \frac{\vec{k}_\perp^2 + m_{\bar{q}}^2}{1-x}}_{\text{LF kinetic energy}} + \underbrace{\kappa^4 \zeta^2}_{\text{longitudinal confinement}} - \underbrace{\frac{\kappa^4}{(m_q + m_{\bar{q}})^2} \partial_x (x(1-x) \partial_x)}_{\text{one-gluon exchange}} + \underbrace{V_g}_{\text{dilation field } \sim e^{-\kappa^2 z^2}}$$

dilation field $\sim e^{-\kappa^2 z^2}$
new for heavy quarkonium!

Working Month 2016, Beijing, China



Confining Potential

Semi-Classical Light-Front Schrödinger equation:

[Brodsky '05]

$$\left[\frac{\vec{k}_\perp^2 + m_q^2}{x(1-x)} + V(\vec{k}_\perp, x) \right] \psi_{h/q\bar{q}}(\vec{k}_\perp, x) = M_h^2 \psi_{h/q\bar{q}}(\vec{k}_\perp, x)$$

► Holographic QCD or AdS/QCD

[e.g., Erlich '05, Karch '06]

► inspired by the string/gauge duality or AdS/CFT

[Maldacena '98]

► fields in AdS_5 directly matched to hadrons

► introduce dilaton field $\varphi(z)$ to break the conformal symmetry
soft-wall model: $\varphi(z) \sim \kappa^2 z^2$ produces the Regge trajectory

► Light-Front Holography relates the semi-classical LF Schrödinger equation to AdS/QCD

[Brodsky '06–'15]

$$\begin{aligned} \zeta_\perp \triangleq \sqrt{x(1-x)} \vec{r}_\perp &\longleftrightarrow z \quad (\text{the 5}^{\text{th}} \text{ dimension}) \\ V &\longleftrightarrow \frac{1}{2} \varphi''(z) + \frac{1}{4} \varphi'^2(z) - \frac{3}{2z} \varphi'(z) \end{aligned}$$

- the soft-wall confining potential: $V(\zeta_\perp) = \kappa^4 \zeta_\perp^2 + \text{const.}$
- connection established for arbitrary spin mesons and baryons
- application: spectrum, form factors, β -function, ...



The Hamiltonian is analytically solvable without the one-gluon exchange:

- ▶ transverse: 2D HO in holographic variables $\phi_{nm}(\vec{k}_\perp/\sqrt{x(1-x)})$
- ▶ longitudinal: $\chi_\ell(x) = x^{\frac{1}{2}\alpha}(1-x)^{\frac{1}{2}\beta}P_\ell^{(\alpha,\beta)}(2x-1)$
 $\alpha = 2m_{\bar{q}}(m_q + m_{\bar{q}})/\kappa^2$, $\beta = 2m_q(m_q + m_{\bar{q}})/\kappa^2$, $P_\ell^{(a,b)}(z)$ Jacobi polynomials
- ▶ mass eigenvalues:

$$M_{nm\ell}^2 = (m_q + m_{\bar{q}})^2 + 2\kappa^2(2n + |m| + \ell + 3/2) + \frac{\kappa^4}{(m_q + m_{\bar{q}})^2}\ell(\ell + 1)$$

We adopt these functions (soft-wall LFWFs) as the basis:

$$\psi_{h/q\bar{q}}(\vec{k}_\perp, x, s, \bar{s}) = \sum_{n,m,l} \Psi_{h/q\bar{q}}(n, m, l, s, \bar{s}) \phi_{nm}\left(\frac{\vec{k}_\perp}{\sqrt{x(1-x)}}\right) \chi_l(x)$$

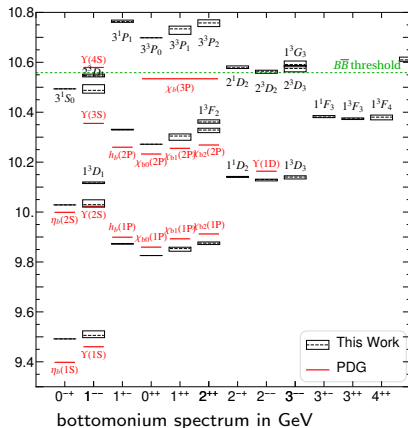
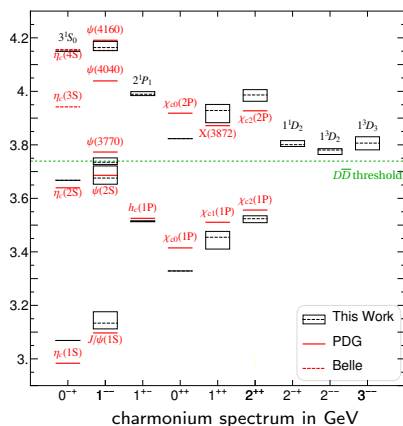
- ▶ implement LF holographic QCD for first approximation
- ▶ transverse 2D HO functions are scalable in the many-body sector (factorization of c.m. motion)
- ▶ basis truncation: $2n + |m| + 1 \leq N_{\max}$, $l \leq L_{\max}$
- ▶ quantum number identification (esp. mirror parity)

[YL '13]

[Soper '72]

We fix α_s and fit κ , m_q to the experimentally measured masses.

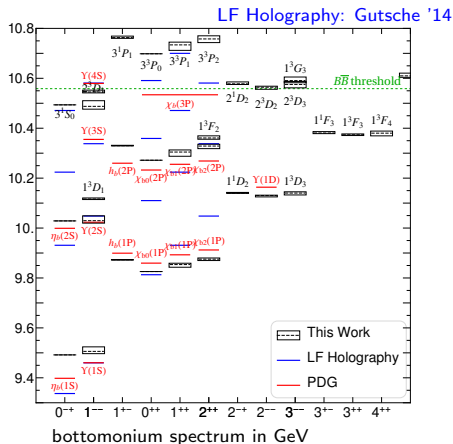
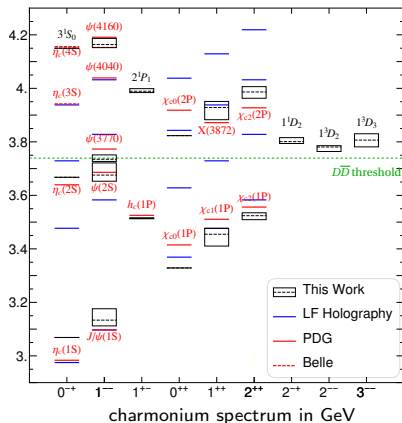




Masses show weak m_J dependence due to the violation of rotational symmetry. We use boxes to indicate the spread of masses (dashed bars: averaged masses).

	α_s	μ_g (GeV)	κ (GeV)	m_q (GeV)	$\delta\overline{M}$ (MeV)	$N_{\max} = L_{\max}$
$c\bar{c}$	0.3595	0.02	0.938	1.522	52 (8 states)	24
$b\bar{b}$	0.2500		1.490	4.763	50 (14 states)	





Masses show weak m_J dependence due to the violation of rotational symmetry. We use boxes to indicate the spread of masses (dashed bars: averaged masses).

	α_s	μ_g (GeV)	κ (GeV)	m_q (GeV)	$\delta\overline{M}$ (MeV)	$N_{\max} = L_{\max}$
$c\bar{c}$	0.3595	0.02	0.938	1.522	52 (8 states)	24
$b\bar{b}$	0.2500		1.490	4.763	50 (14 states)	

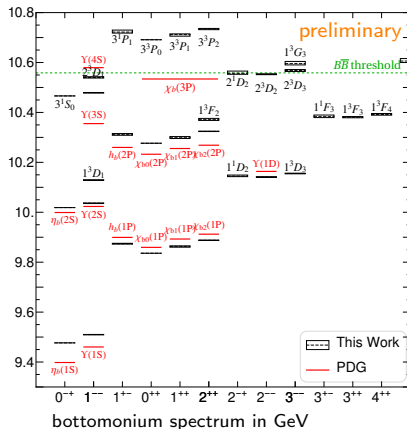
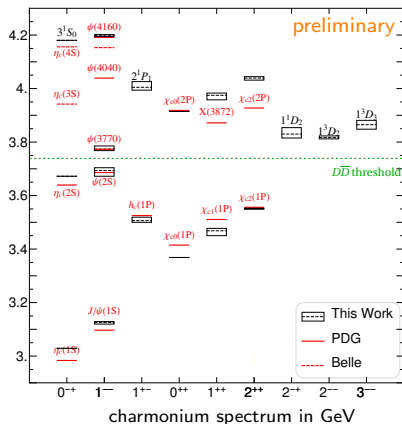


Mass Spectroscopy: Improvement

[work in progress]

Running coupling implements important UV physics:

$$\alpha_s(Q^2) = \frac{\alpha_s(M_Z^2)}{1 + \alpha_s(M_Z^2)\beta_0 \ln\left(\frac{\mu_{\text{IR}}^2 + Q^2}{\mu_{\text{IR}}^2 + M_Z^2}\right)}, \quad V_g = -\frac{4}{3} \times \frac{4\pi\alpha_s(Q^2)}{Q^2} \bar{u}_\sigma \gamma^\mu u_\sigma \bar{v}_s \gamma_\mu v_{s'}$$



The running coupling improves the one-gluon exchange kernel. The m_J -dependence of masses becomes weaker. The overall mass spectrum is improved: $\delta\bar{M} = 28$ MeV (charmonium) 43 MeV (bottomonium) ($N_{\text{max}} = L_{\text{max}} = 16$, $\alpha_s(0) = 0.6$)



Model Parameters and Regulator Sensitivity

- ▶ For HO basis, $\Omega_{\text{IR}} \sim b/\sqrt{N_{\text{max}}}$, $\Omega_{\text{UV}} \sim b\sqrt{N_{\text{max}}}$. [Coon '12]
- ▶ Positronium: continuum limit $N_{\text{max}} \rightarrow \infty$, $L_{\text{max}} \rightarrow \infty$, $\mu_g \rightarrow 0$ can be reached through successive extrapolations. [Wiecki '15, Vary '15]
- ▶ Quarkonium, $N_{\text{max}} = L_{\text{max}} = 8, 16, 24$
 - ▶ κ, m_q refitted and turned out to be very close ($\lesssim 1\%$ changes).
 - ▶ The r.m.s. mass deviations are also comparable.

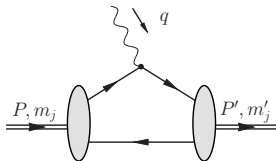
	α_s	μ_g (GeV)	κ (GeV)	m_q (GeV)	$\delta\overline{M}$ (MeV)	N_{max}
$c\bar{c}$	0.3595	0.02	0.963	1.492	56 (8 states)	8
$b\bar{b}$	0.2500		1.492	4.758	55 (14 states)	
$c\bar{c}$	0.3595	0.02	0.950	1.510	52 (8 states)	16
$b\bar{b}$	0.2500		1.491	4.761	51 (14 states)	
$c\bar{c}$	0.3595	0.02	0.938	1.522	52 (8 states)	24
$b\bar{b}$	0.2500		1.490	4.763	50 (14 states)	
$c\bar{c}$	$\alpha_s(Q)$	0.02	0.979	1.587	28 (8 states)	16
$b\bar{b}$			1.451	4.890	43 (14 states)	

preliminary



Charge Form Factors

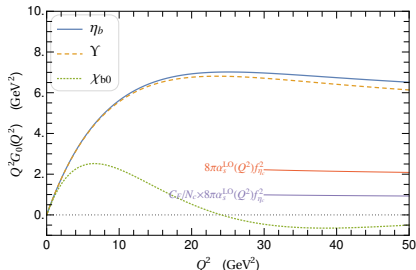
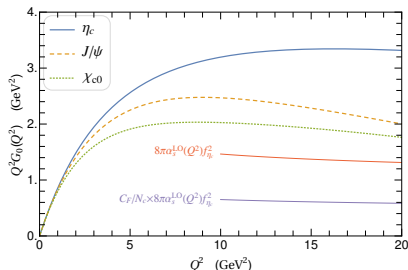
[YL et al., Phys.Lett.B **758**, 118 (2016)]



Form factors are defined from the matrix elements of the “good current”,

$$I_{\lambda,\lambda'}^+(Q^2) = \langle P', \lambda' | J^+(0) | P, \lambda \rangle / (2P^+),$$

where $q = P' - P$, $Q^2 = -q^2$.



- ▶ Impulse approximation with only the two-body contribution.
- ▶ GK prescription for (axial-)vectors
- ▶ pQCD asymptotics: $Q^2 F_P(Q^2) \sim 8\pi\alpha_s f_P^2$

[Grach '84]

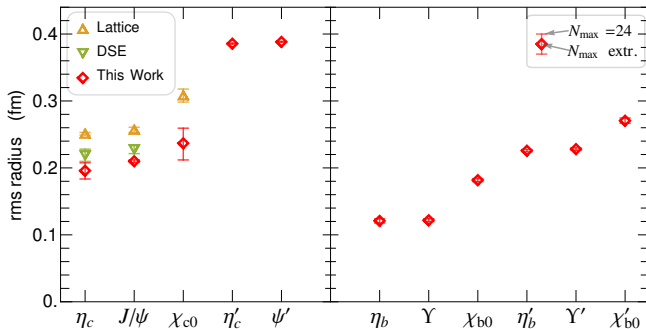
[Lepage & Brodsky '80]



The charge radius:

$$\langle r^2 \rangle = -6 \frac{\partial}{\partial Q^2} G_0(Q^2) \Big|_{Q^2 \rightarrow 0}.$$

- test long-distance physics (cf. decay constants)



[DSE: Maris '07; Lattice: Dudeck '06]

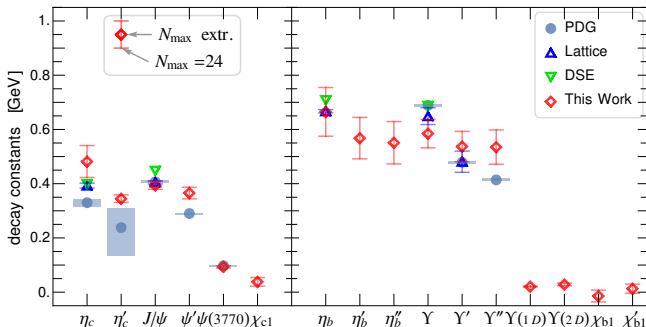
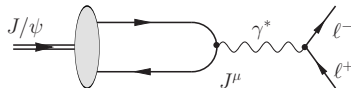


Decay Constants

[YL et al., Phys.Lett.B 758, 118 (2016)]

$$\langle 0 | \bar{\psi} \gamma^\mu \gamma^5 \psi | P(p) \rangle = i p^\mu f_P,$$

$$\langle 0 | \bar{\psi} \gamma^\mu \psi | V_\lambda(p) \rangle = e_\lambda^\mu(p) m_V f_V$$



[DSE: Blank '11, Lattice: HPQCD, '10-'15]

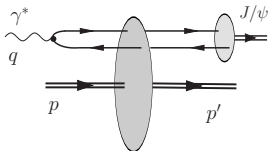
- ▶ Test “wavefunction at the origin” (cf. charge radius)
- ▶ Results are in reasonable agreement with experimental measurements as well as Lattice and DSE calculations where available.
- ▶ Results were extrapolated from $N_{\max} = L_{\max} = 8, 16, 24$, and there is some residual regulator dependence.



Diffractive Vector Meson Production

[Chen, in preparation]

Diffractive VM production in DIS is an important tool for studying the small- x gluon distribution at a future Electron-Ion Collider.



In color dipole picture:

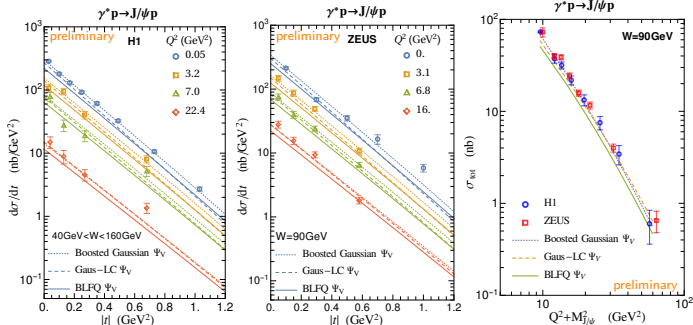
$$\mathcal{A}_{T,L}^{\gamma^* p \rightarrow V p} = \int d^2 r_{\perp} \int \frac{dz}{4\pi} [\psi_V \psi]_{T,L} \mathcal{A}_{q\bar{q}}(z, \vec{r}_{\perp}, \Delta_{\perp})$$

$(\psi_V \psi)_{T,L}$: overlap of photon/vector meson LFWFs

[Mueller '94, Nikolaev '91]

Initial study: ep collision with IP-Sat for $\mathcal{A}_{q\bar{q}}$

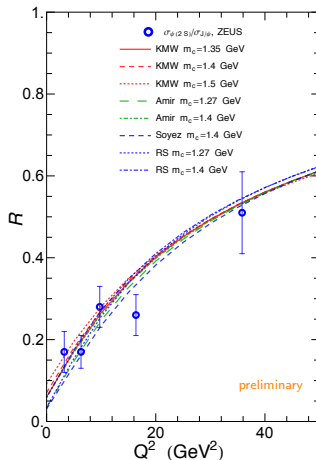
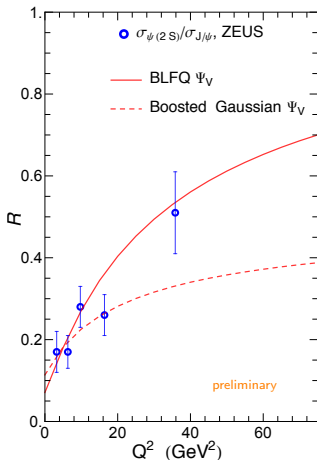
[Kowalski, Teaney '03]



ψ_V : boosted Gaussian, Gaus-LC ($m_c = 1.4 \text{ GeV}$) vs. BLFQ ($m_c = 1.35 \text{ GeV}$)



The diffractive VM production tests BLFQ over a dynamical range not covered by the mass spectroscopy and decay constants.



Provides access to excited states that are well constrained by physical observables (mass spectrum, decay constant etc).



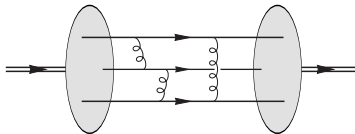
Generalization to Baryons

[work in progress]

The effective interaction can be generalized to the baryon sector:

$$H_{\text{eff}} = \sum_a \frac{\vec{p}_{a\perp}^2 + m_a^2}{x_a} - \vec{P}_\perp^2 + \frac{1}{2} \sum V_{ab}^{(2)} + \frac{1}{6} \sum_{a,b,c} V_{abc}^{(3)} + \dots$$

- ▶ The soft-wall confinement: $V_{\text{SW}} = \frac{1}{2} \sum_{a,b} x_a x_b (\vec{r}_{a\perp} - \vec{r}_{b\perp})^2$.
- ▶ The one-gluon exchange



Jacobi coordinates on the light front (three-body example):

longitudinal: $x = x_3$, $\chi = \frac{x_2}{1-x_3}$;

transverse momenta: $\vec{k}_\perp = (1-x_3)\vec{p}_{3\perp} - x_3(\vec{p}_{1\perp} + \vec{p}_{2\perp})$, $\vec{\kappa}_\perp = \frac{x_1\vec{p}_{2\perp} - x_2\vec{p}_{1\perp}}{x_1+x_2}$;

transverse coordinates: $\vec{r}_\perp = \vec{r}_{3\perp} - \frac{x_1\vec{r}_{1\perp} - x_2\vec{r}_{2\perp}}{x_1+x_2}$, $\vec{\rho}_\perp = \vec{r}_{1\perp} - \vec{r}_{2\perp}$.

- ▶ Taking advantage of the kinematical nature of light-front boosts
- ▶ The longitudinal confinement

$$V_L = -\frac{\kappa^4}{(m_1+m_2+m_3)^2} \left[\partial_x (x(1-x)\partial_x) + \frac{1}{1-x} \partial_\chi (\chi(1-\chi)\partial_\chi) \right]$$



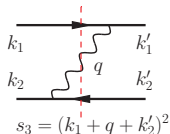
Part III:

Non-Perturbative Renormalization



Hamiltonian perturbation theory: x^+ -ordered diagrams

- ▶ all particles are on their mass-shells $p_i^2 = m_i^2$;
- ▶ longitudinal and transverse momenta are conserved at each vertex;
 $\delta(\sum_i p_i^+ - P^+) \Leftrightarrow \delta(\sum_i -1)$; $\delta^2(\sum_i \vec{p}_{i\perp} - \vec{P}_\perp) \Leftrightarrow \delta^2(\sum_i \vec{k}_{i\perp})$
- ▶ the light-front energy is *not conserved* ("off the energy shell");
- ▶ energy denominator for intermediate states;



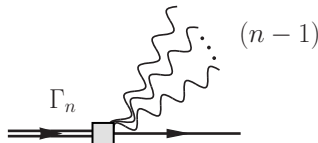
$$\frac{1}{s_n - M^2}, \quad s_n \equiv (k_1 + \dots + k_n)^2 = \sum_{a=1}^n \frac{\vec{k}_{a\perp}^2 + m_a^2}{x_a},$$

M is the mass eigenvalue

Extended to non-perturbative regime by introducing vertex functions Γ_n

$$\Gamma_n = (s_n - M^2)\psi_n.$$

Γ_n are also boost invariants.



Renormalization

- QFT is defined with bare parameters (equivalently, counterterms). Renormalization relates these bare parameters to “physical” quantities. The bare parameters may contain divergences which is allowed as they are not physical observables.
- Renormalization depends on the regularization scheme. Infinities may arise and the theory has to be regularized first.
- After renormalization, the theory should be free of divergences in *all sectors* (e.g. bound states) even in the non-perturbative regime. Ensuring exactly cancellation of divergences (within the numerical precision) in the non-perturbative regime is often a challenge as the solutions often rely on numerical procedures.
- General principles:
 - **Mass renormalization:** imposing the physical mass $M \rightarrow m_{\text{ph}}$
 - **Coupling constant renormalization:** imposing the physical coupling on the vertex $\Gamma_2(\vec{k}_\perp^*, x^*) = g_{\text{ph}} \sqrt{Z}$ at some chosen kinematic point (\vec{k}^*, x^*) .
 - **Wavefunction renormalization:** simply the normalization of the LFWFs! $\sum_n \int dD_n |\psi_n|^2 = 1$



$$\mathcal{L} = \partial_\mu \chi^\dagger \partial^\mu \chi - m^2 \chi^\dagger \chi + \frac{1}{2} \partial_\mu \varphi^\mu - \frac{1}{2} \mu^2 \varphi^2 \\ + g_B \chi^\dagger \chi \varphi + \delta m^2 \chi^\dagger \chi + \frac{1}{2} \delta \mu^2 \varphi^2 + \dots$$

where $m = 0.94 \text{ GeV}$, $\mu = 0.14 \text{ GeV}$, $\alpha \equiv g^2/(16\pi m^2)$. g_B and δm^2 are renormalization parameters yet to be determined.

- ▶ Yukawa potential: $\phi(r) = -\alpha e^{-\mu r}/r$.
- ▶ Pauli-Villars (PV) regularization with PV mass μ_{PV}
- ▶ Vacuum instability
 - ▶ exclude “anti-chion” degrees-of-freedom
 - ▶ similar to the quenched approximation
 - ▶ purely for simplicity (cf. Higgs field)

[Brodsky '01]

[Baym '60]

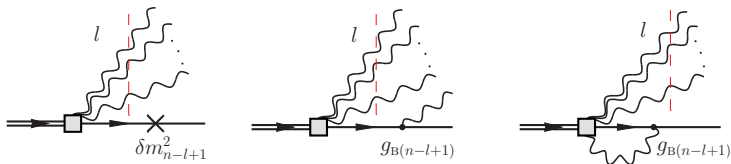
- ▶ Fock sector expansion of a physical “chion” state,
 $|\mathcal{X}\rangle = |\chi\rangle + |\chi\varphi\rangle + |\chi\varphi\varphi\rangle + |\chi\varphi\varphi\varphi\rangle + \dots$

- ▶ Fock sector truncation (“light-front Tamm-Dancoff”)
- ▶ to justify the sector truncation, we compare observables from successive truncations up to four-body ($\chi + 3\varphi$).

[Perry '90]

Yukawa: Karmanov '12, QED: Hiller '98, Karmanov '08, Chabysheva '10





n is the maximum number of dressing bosons allowed by the truncation, l is the number of spectators.

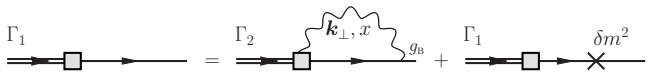
The general Fock sector dependent counterterms:

- ▶ $\delta m_1 = g_{B1} = 0$ (no dressing/coupling allowed by the truncation)
- ▶ $\delta m_2^2, \dots, \delta m_{n+1}^2$ and $g_{B2}, \dots, g_{B(n+1)}$ appear in the $(n+1)$ -body truncation.
- ▶ The sector dependent counterterms are determined inductively.
e.g., 2-body truncation \rightarrow 3-body truncation \rightarrow 4-body truncation ...
- ▶ Resemblance to the perturbative renormalization

[Zimmermann '69]



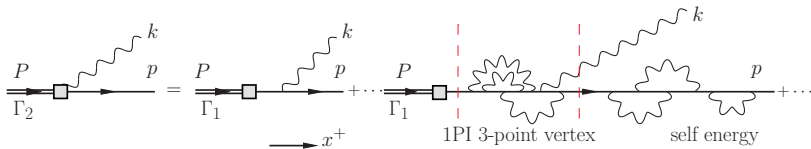
Mass renormalization condition:



$$0 = \sum_{j=0}^1 (-1)^j \int_0^1 \frac{dx}{2x(1-x)} \int \frac{d^2 k_\perp}{(2\pi)^3} g_{Bn} \psi_2^{j(n)}(\mathbf{k}_\perp, x) + \delta m^2 \psi_1^{(n)}.$$

Coupling constant renormalization:

[Karmanov '10]



$$\Gamma_2 = \Gamma_1 + \dots + \text{1PI 3-point vertex} + \text{self energy} + \dots$$

$\longrightarrow x^+$

$$\forall x \in (0, 1), \quad \Gamma_2^{0(n)}(\mathbf{k}_\perp^*, x) = g \sqrt{I_1^{(n-1)}}, \quad \left(\frac{\mathbf{k}^{*2}}{x} + \frac{\mathbf{k}^{*2} + \mu^2}{1-x} = m^2 \right).$$

Wavefunction/field strength renormalization $I_1 + I_2 + \dots + I_n = 1$,

where $I_l = \int dD_l |\psi_l(k_1, k_2, \dots, k_l)|^2$.



Eigenvalue Equation

The diagram illustrates the eigenvalue equation for a fermion propagator with a mass insertion. The equation is written as a sum of diagrams on the left equals a sum of diagrams on the right.

Left side (LHS):

- Diagram 1: A fermion line with a square mass insertion vertex. The incoming line is labeled Γ_1 .
- Diagram 2: A fermion line with a square mass insertion vertex. The incoming line is labeled Γ_2 . A wavy line (representing a boson) is attached to the vertex.
- Diagram 3: A fermion line with a square mass insertion vertex. The incoming line is labeled Γ_3 . Two wavy lines are attached to the vertex, labeled a and b .
- Diagram 4: A fermion line with a square mass insertion vertex. The incoming line is labeled Γ_4 . Three wavy lines are attached to the vertex, labeled a , b , and c .

Right side (RHS):

- Diagram 1: A fermion line with a square mass insertion vertex. The incoming line is labeled Γ_1 . The vertex is crossed out with an 'X'. The label δm^2 is below the vertex.
- Diagram 2: A fermion line with a square mass insertion vertex. The incoming line is labeled Γ_2 . A wavy line is attached to the vertex. The label g_B is below the vertex.
- Diagram 3: A fermion line with a square mass insertion vertex. The incoming line is labeled Γ_1 . A wavy line is attached to the vertex. The label g_B is below the vertex.
- Diagram 4: A fermion line with a square mass insertion vertex. The incoming line is labeled Γ_2 . The vertex is crossed out with an 'X'. The label δm^2 is below the vertex.
- Diagram 5: A fermion line with a square mass insertion vertex. The incoming line is labeled Γ_3 . A wavy line is attached to the vertex. The label g_B is below the vertex.
- Diagram 6: A fermion line with a square mass insertion vertex. The incoming line is labeled Γ_2 . Two wavy lines are attached to the vertex, labeled a and b . The label g_B is below the vertex.
- Diagram 7: A fermion line with a square mass insertion vertex. The incoming line is labeled Γ_2 . Two wavy lines are attached to the vertex, labeled a and b . The label g_B is below the vertex.
- Diagram 8: A fermion line with a square mass insertion vertex. The incoming line is labeled Γ_3 . Two wavy lines are attached to the vertex, labeled a and b . The vertex is crossed out with an 'X'. The label δm^2 is below the vertex.
- Diagram 9: A fermion line with a square mass insertion vertex. The incoming line is labeled Γ_4 . Three wavy lines are attached to the vertex, labeled a , b , and c . The label g_B is below the vertex.
- Diagram 10: A fermion line with a square mass insertion vertex. The incoming line is labeled Γ_3 . Three wavy lines are attached to the vertex, labeled a , b , and c . The label g_B is below the vertex.

The equation is written as:

$$\text{LHS} = \text{RHS}$$

The RHS is a sum of the diagrams listed above, with the last three terms grouped as $(a \leftrightarrow b) + (a \leftrightarrow c) + \dots$.



Eigenvalue Equation

2-body truncation

$$\begin{aligned}
 \Gamma_1 &= \Gamma_1 \times \delta m^2 + \Gamma_2 g_B \\
 \Gamma_2 &= \Gamma_1 g_B + \Gamma_2 \times \delta m^2 \\
 &+ \Gamma_3 g_B \\
 \Gamma_3 &= \Gamma_2 g_B + \Gamma_2 \times \delta m^2 + \Gamma_4 g_B \\
 \Gamma_4 &= \Gamma_3 g_B + (a \leftrightarrow b) + (a \leftrightarrow c) + \dots
 \end{aligned}$$



Eigenvalue Equation

Diagrammatic equations for the eigenvalue equation, showing the truncation of the 3-body term.

3-body truncation

The equations are organized into rows, each representing a different order of the expansion. The first row shows the truncation of the 3-body term, and the subsequent rows show the truncation of the 4-body term.

Row 1 (3-body truncation):

$$\Gamma_1 \text{ (diagram)} = \Gamma_1 \text{ (diagram)} \times \delta m^2 + \Gamma_2 \text{ (diagram)} g_B$$

Row 2 (3-body truncation):

$$\Gamma_2 \text{ (diagram)} = \Gamma_1 \text{ (diagram)} g_B + \Gamma_2 \text{ (diagram)} \times \delta m^2$$

Row 3 (3-body truncation):

$$\Gamma_3 \text{ (diagram)} = \Gamma_2 \text{ (diagram)} g_B + \Gamma_3 \text{ (diagram)} g_B$$

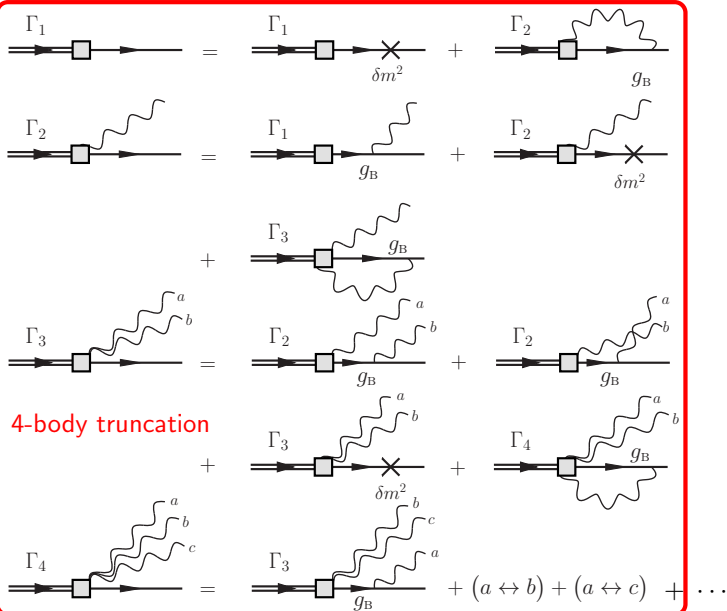
Row 4 (4-body truncation):

$$\Gamma_4 \text{ (diagram)} = \Gamma_3 \text{ (diagram)} g_B + (a \leftrightarrow b) + (a \leftrightarrow c) + \dots$$

The diagrams use double lines for fermions, single lines for bosons, and wavy lines for gluons. The vertices are represented by squares. The labels $\Gamma_1, \Gamma_2, \Gamma_3, \Gamma_4$ indicate the order of the expansion. The labels δm^2 and g_B indicate the mass and coupling constants. The labels a, b, c indicate the external lines.



Eigenvalue Equation



Two- and Three-Body Truncations [YL et al., Phys.Lett.B **758**, 118 (2016)]

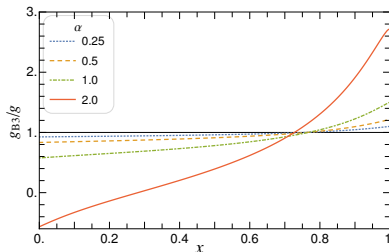
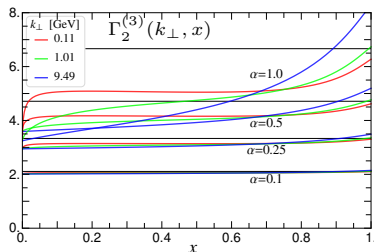
Two-body truncation solution is equivalent to the leading order perturbation theory.

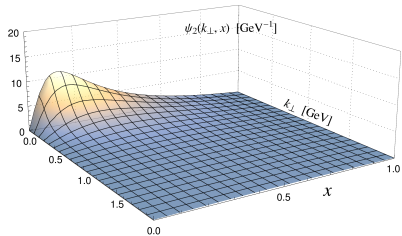
$$\Gamma_2^{j(2)}(\mathbf{k}_\perp, x) = g, \quad \psi_2^{j(2)}(\mathbf{k}_\perp, x) = g/(s_2 - m^2).$$

- ▶ Landau pole for $\alpha > \alpha_L \approx 2.63$

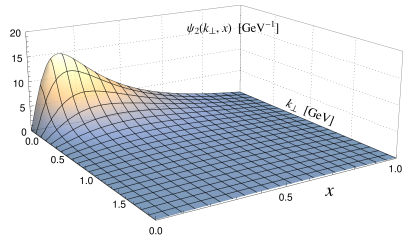
Three-body truncation is solved numerically from a linear inhomogeneous integral equation.

- ▶ Bare coupling “constant” g_{B3} depends on x , as a consequence of the violation of the Lorentz symmetry. [Karmanov '12]
- ▶ Fredholm singularity at $\alpha = \alpha_F \approx 2.19$

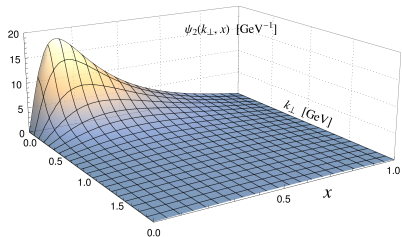




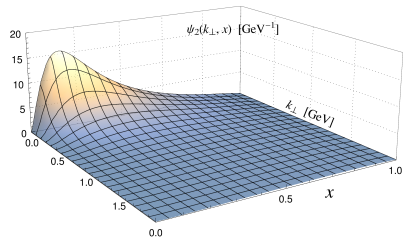
$\alpha = 0.25$



$\alpha = 0.5$



$\alpha = 1.0$

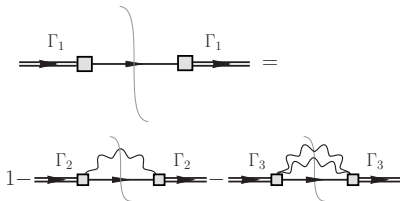


$\alpha = 2.0$

The two-body LFWF $\psi_2(k_\perp, x)$ at selected couplings



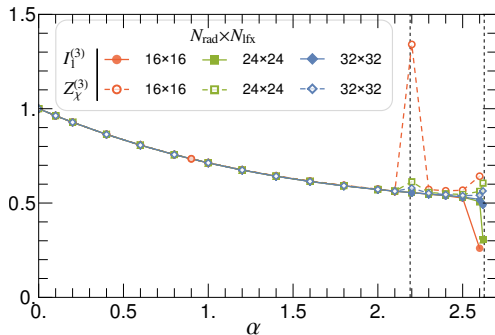
An important cross-check is the relation $I_1 = Z_\chi$ in three-body:



$$\Sigma(p^2) = \frac{p}{\Gamma_2/\sqrt{I_1}} \text{ (diagram with } \mathbf{k}_\perp, x \text{ and } g_B \text{) }$$

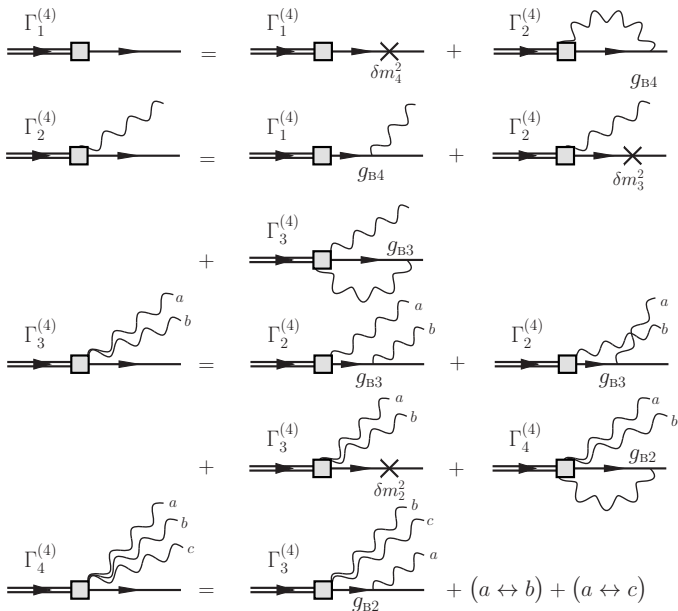
$$Z_\chi = \left[1 - \frac{\partial}{\partial p^2} \Sigma(p^2) \right]_{p^2 \rightarrow m^2}^{-1}$$

Non-perturbative, numerically evaluated:



Four-Body Truncation

[YL et al., Phys.Lett.B **758**, 118 (2016)]

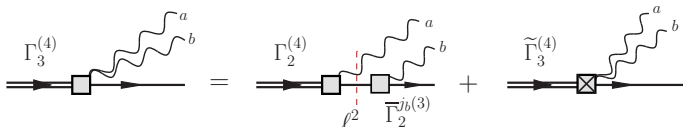


$$\Gamma_2^{j(4)}(\mathbf{k}_\perp, x) = g_{B4} \psi_1^{(4)} + \frac{\delta m_3^2}{1-x} \frac{\Gamma_2^{j(4)}(\mathbf{k}_\perp, x)}{s_2 - m^2} + \sum_{j'=0}^1 (-1)^{j'} \int_0^{1-x} \frac{dx'}{2x'(1-x-x')} \int \frac{d^2 k'_\perp}{(2\pi)^3} g_{B3}(\frac{x'}{1-x}) \psi_3^{jj'(4)}(\mathbf{k}_\perp, x, \mathbf{k}'_\perp, x'),$$

- ▶ The renormalization conditions have to be imposed numerically.
- ▶ On-Shell coupling constant renormalization gives mass poles

$$\psi_2^{0(4)}(\mathbf{k}_\perp^\star, x) \sim \lim_{s_2^\star \rightarrow m^2} \frac{1}{s_2^\star - m^2}, \quad \psi_3^{0j'(4)}(\mathbf{k}_\perp^\star, x, \mathbf{k}'_\perp, x') \sim \lim_{s_2^\star \rightarrow m^2} \frac{1}{s_2^\star - m^2}.$$

- ▶ Isolate the singularities:

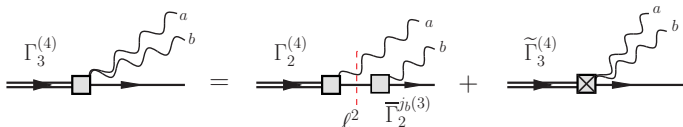


$$\Gamma_2^{0(4)}(\mathbf{k}_\perp^*, x) = g_{B4} \psi_1^{(4)} + \frac{\delta m_3^2}{1-x} \frac{\Gamma_2^{0(4)}(\mathbf{k}_\perp^*, x)}{s_2^* - m^2} + \sum_{j'=0}^1 (-1)^{j'} \int_0^{1-x} \frac{dx'}{2x'(1-x-x')} \int \frac{d^2 k'_\perp}{(2\pi)^3} g_{B3}(\frac{x'}{1-x}) \psi_3^{0j'(4)}(\mathbf{k}_\perp^*, x, \mathbf{k}'_\perp, x'),$$

- The renormalization conditions have to be imposed numerically.
- On-Shell coupling constant renormalization gives mass poles

$$\psi_2^{0(4)}(\mathbf{k}_\perp^*, x) \sim \lim_{s_2^* \rightarrow m^2} \frac{1}{s_2^* - m^2}, \quad \psi_3^{0j'(4)}(\mathbf{k}_\perp^*, x, \mathbf{k}'_\perp, x') \sim \lim_{s_2^* \rightarrow m^2} \frac{1}{s_2^* - m^2}.$$

- Isolate the singularities:



Four-Body Truncation

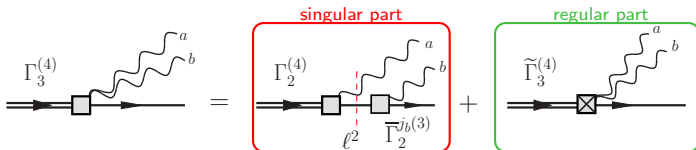
[YL et al., Phys.Lett.B **758**, 118 (2016)]

$$\Gamma_2^{0(4)}(\mathbf{k}_\perp^*, x) = g_{B4} \psi_1^{(4)} + \frac{\delta m_3^2}{1-x} \frac{\Gamma_2^{0(4)}(\mathbf{k}_\perp^*, x)}{\textcolor{red}{s}_2^* - m^2} + \sum_{j'=0}^1 (-1)^{j'} \int_0^{1-x} \frac{dx'}{2x'(1-x-x')} \int \frac{d^2 k'_\perp}{(2\pi)^3} g_{B3}(\frac{x'}{1-x}) \textcolor{red}{\psi}_3^{0j'(4)}(\mathbf{k}_\perp^*, x, \textcolor{red}{\mathbf{k}}'_\perp, x'),$$

- ▶ The renormalization conditions have to be imposed numerically.
- ▶ On-Shell coupling constant renormalization gives mass poles

$$\psi_2^{0(4)}(\mathbf{k}_\perp^*, x) \sim \lim_{s_2^* \rightarrow m^2} \frac{1}{s_2^* - m^2}, \quad \psi_3^{0j'(4)}(\mathbf{k}_\perp^*, x, \mathbf{k}'_\perp, x') \sim \lim_{s_2^* \rightarrow m^2} \frac{1}{s_2^* - m^2}.$$

- ▶ Isolate the singularities:

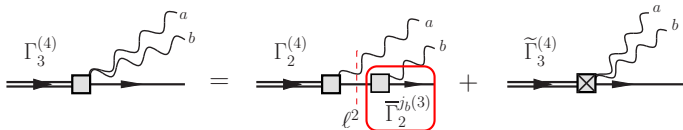


$$\Gamma_2^{0(4)}(\mathbf{k}_\perp^*, x) = g_{B4} \psi_1^{(4)} + \frac{\delta m_3^2}{1-x} \frac{\Gamma_2^{0(4)}(\mathbf{k}_\perp^*, x)}{\mathbf{s}_2^* - m^2} + \sum_{j'=0}^1 (-1)^{j'} \int_0^{1-x} \frac{dx'}{2x'(1-x-x')} \int \frac{d^2 k'_\perp}{(2\pi)^3} g_{B3}(\frac{x'}{1-x}) \psi_3^{0j'(4)}(\mathbf{k}_\perp^*, x, \mathbf{k}'_\perp, x'),$$

- The renormalization conditions have to be imposed numerically.
- On-Shell coupling constant renormalization gives mass poles

$$\psi_2^{0(4)}(\mathbf{k}_\perp^*, x) \sim \lim_{s_2^* \rightarrow m^2} \frac{1}{s_2^* - m^2}, \quad \psi_3^{0j'(4)}(\mathbf{k}_\perp^*, x, \mathbf{k}'_\perp, x') \sim \lim_{s_2^* \rightarrow m^2} \frac{1}{s_2^* - m^2}.$$

- Isolate the singularities:



- Inhomogeneous linear coupled integral equations
- Approximate the integrals by Gauss-Legendre quadratures
$$d \sim N_{\text{rad}}^2 N_{\text{ang}} N_{\text{lfx}}^2$$
- Implement an iterative procedure in Fortran w. MPI/OpenMP typically 50 ~ 100 iterations
- Numerical calculation on Hopper at NERSC
largest single run: 1680 cores \times 18 hours

A representative two-body LFWF, $\psi_2(k_{\perp}, x)$:

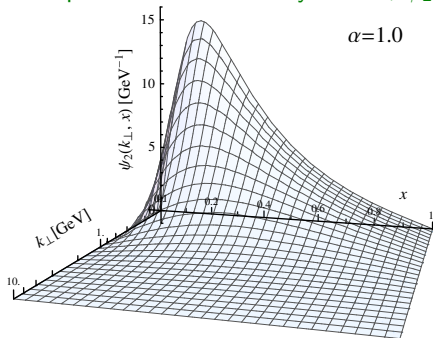


Image credit: NERSC

$\alpha = 1.0$, $m = 0.94\text{GeV}$,
 $\mu = 0.14\text{GeV}$, $\mu_{\text{PV}} = 15\text{GeV}$

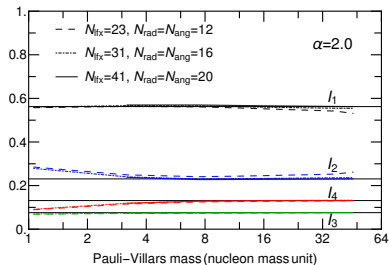
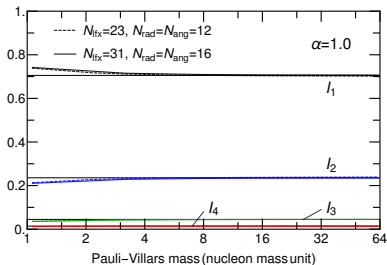
Grid size:

$N_{\text{lfx}} = 47$, $N_{\text{rad}} = N_{\text{ang}} = 20$



UV Convergence

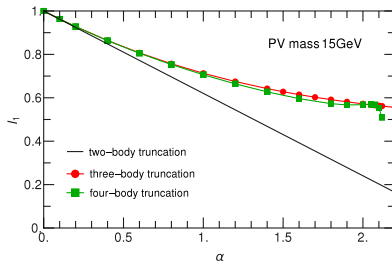
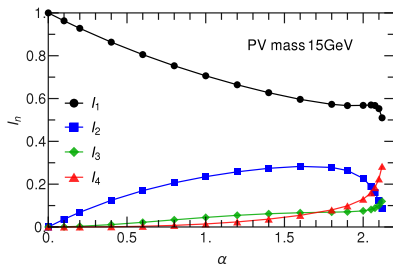
[YL et al., Phys.Lett.B **758**, 118 (2016)]



- ▶ I_n well converge with respect to μ_{PV} for sufficiently fine grid.
- ▶ Large coupling α or large Pauli-Villars mass μ_{PV} may need finer grid to achieve convergence.
- ▶ In our calculation, the grid is independent of μ_{PV} .
In practice, UV regulator-dependent meshes are widely used.
- ▶ In practice, we take $\mu_{\text{PV}} = 15 \text{ GeV}$ with the numbers of grid points $N_{\text{fix}} = 41, N_{\text{rad}} = N_{\text{ang}} = 20$.



$$I_n \equiv \int D_n |\psi_n(k_1, k_2, \dots, k_n; p)|^2, \quad \sum_n I_n = 1.$$



- ▶ For $\alpha \lesssim 1.7$, there exists a sector hierarchy $I_1 > I_2 > I_3 > I_4$. One- & two-body contributions dominate. $I_{n>4}$ are negligible.
- ▶ $\alpha_L \approx 2.6$, $\alpha_F \approx 2.2$
- ▶ I_1 saturates in the four-body truncation up to $\alpha \approx 2.0$.



Electromagnetic Form Factor

[YL et al., Phys.Lett.B **758**, 118 (2016)]

Form factors are defined as the current matrix element, as mentioned:

$$\langle \psi(p+q) | J^+(0) | \psi(p) \rangle = 2p^+ F(Q^2)$$

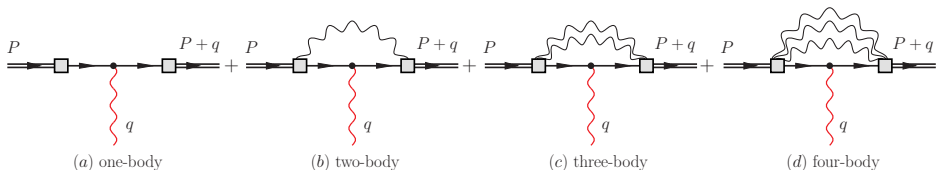
where $q^+ = 0$ and $Q^2 = -q^2 = \mathbf{q}_\perp^2 > 0$, and the e.m. current:

$$J^\mu = i(D^\mu \chi)^\dagger \chi - i\chi^\dagger D^\mu \chi.$$

- Drell-Yan-West formula (overlap of LFWFs)

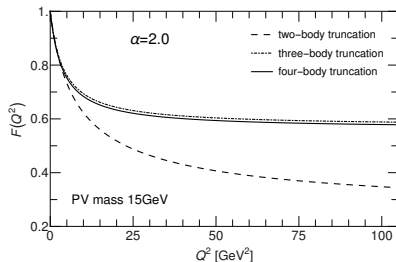
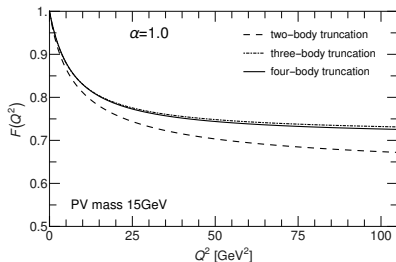
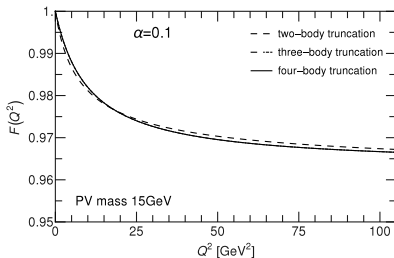
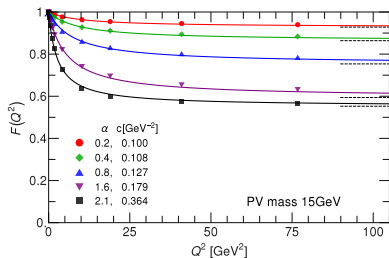
$$F(Q^2) = \sum_n \int dD_n \psi_n^* (\{\mathbf{k}'_{i\perp}, x_i\}) \psi_n (\{\mathbf{k}_{i\perp}, x_i\}_n);$$

- The n-body contribution $F_n(Q^2 \rightarrow 0) \rightarrow I_n$
- $F(Q^2 \rightarrow 0) \rightarrow 1$ — charge conservation
- $F(Q^2 \rightarrow \infty) \rightarrow I_1$ — point-like charge



Electromagnetic Form Factor

[YL et al., Phys.Lett.B **758**, 118 (2016)]



Electromagnetic form factor saturates as the number of constituents increase, even with non-perturbative couplings.



Summary and Outlook

- ▶ Light-Front Hamiltonian formalism is a natural framework for solving non-perturbative relativistic bound-state problems.
- ▶ We demonstrate basis light-front quantization as a computational implementation of LF Hamiltonian approach in electron, positronium and quarkonium problems.
- ▶ We present a systematic non-perturbative renormalization scheme within the LF Hamiltonian formalism in a scalar model.
- ▶ Many of the calculations can be extended to other systems, and, hopefully, eventually to QCD. However, several challenges have to be addressed.
- ▶ My work is a first step to build a systematic computational framework to solve QFTs eps. QCD bound-state problems in an *ab initio* LF Hamiltonian approach.

Thank you!



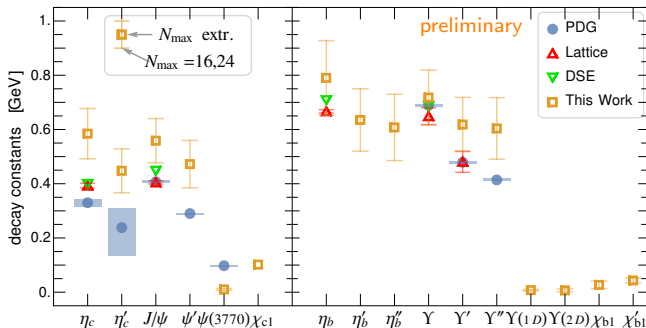


Fin

[Click here to proceed to backup slides...](#)

Decay Constants with Running Coupling

Decay constants with running coupling (with IR modeling)



- ▶ Similar quality but the residual regulator dependence is somewhat stronger.
- ▶ HO basis is designed for confinement (IR) and is expected to have a slower convergence at UV.
- ▶ Need larger N_{\max} , L_{\max} and a careful study of the UV asymptotics of the LFWFs.
- ▶ Renormalization

